



Geophysical Research Letters

RESEARCH LETTER

10.1029/2018GL079464

Key Points:

- A radiocarbon-based estimate of CO₂ absorption rates in the central Amundsen Sea Polynya is 45 ± 20 mmol m⁻² d⁻¹, comparable to values determined by pCO₂ measurements
- The turnover time of water in the western Amundsen Sea is estimated to be a few decades
- Ten to thirty percent of intruding Modified Circumpolar Deep Water along the Dotson Trough mixes with overlying water

Supporting Information:

· Supporting Information S1

Correspondence to:

J. Hwang, ieomshik@snu.ac.kr

Citation:

Kim, B., Lee, S. H., Kim, M., Hahm, D., Rhee, T. S., & Hwang, J. (2018). An investigation of gas exchange and water circulation in the Amundsen Sea based on dissolved inorganic radiocarbon. *Geophysical Research Letters*, 45, 12,368–12,375. https://doi. org/10.1029/2018GL079464

Received 10 JUL 2018 Accepted 25 OCT 2018 Accepted article online 31 OCT 2018 Published online 20 NOV 2018

An Investigation of Gas Exchange and Water Circulation in the Amundsen Sea Based On Dissolved Inorganic Radiocarbon

Bumsoo Kim¹, SangHoon Lee², Minkyoung Kim¹, Doshik Hahm³, Tae Siek Rhee², and Jeomshik Hwang¹

¹School of Earth and Environmental Sciences/Research Institute of Oceanography, Seoul National University, Seoul, South Korea, ²Korea Polar Research Institute, Incheon, South Korea, ³Department of Oceanography, Pusan National University, Busan, South Korea

Abstract We used radiocarbon isotope ratios in dissolved inorganic carbon to assess gas exchange and water circulation in the western Amundsen Sea. Radiocarbon isotope ratios indicate that Circumpolar Deep Water enters the basin along the seafloor and that the upper layer is formed through modification of this water mass. In the Amundsen Sea Polynya, radiocarbon isotope ratios of surface water are higher than those of underlying Winter Water, implying rapid absorption of atmospheric CO_2 . A CO_2 absorption rate of 45 mmol m⁻² d⁻¹ calculated for a site in the central polynya is higher than that near the Dotson Ice Shelf (28 mmol m⁻² d⁻¹). The turnover time of water in the Dotson Trough region of the western Amundsen Sea is estimated to be 10–30 years, based on results from a box model and radiocarbon mass balance.

Plain Language Summary The western Amundsen Sea is experiencing raid physical changes including rapid glacial melting and declining sea ice cover. The suggested heat source is the intrusion of warm Circumpolar Deep Water (CDW) along the seafloor of the Amundsen Shelf. Therefore, understanding the behavior of the intruded CDW, especially how long it stays on the shelf, is important. Physical oceanographic studies have examined the flux of CDW onto and out of the Amundsen Shelf. However, the turnover time of water in the Amundsen Sea is still poorly understood. In this paper, we use radiocarbon isotope signature from dissolved inorganic carbon to examine how rapidly atmospheric CO₂ is absorbed into the Amundsen Sea Polynya and how long the water should stay in the western Amundsen Shelf to have the observed radiocarbon isotope signature. Based on our results and the current understanding of the water circulation in the western Amundsen Sea, we found that the water sits on the Amundsen Shelf for a few decades before it moves off shelf.

1. Introduction

The Amundsen Sea is experiencing rapid physical changes including rapid melting of the ice shelf, retreat of glacier grounding lines, and a decline in sea ice cover (Pritchard et al., 2012; Rignot et al., 2014; Stammerjohn et al., 2012). The intrusion of Circumpolar Deep Water (CDW) is a major source of heat (Wåhlin et al., 2010; Walker et al., 2007), and several studies have examined the intrusion of CDW and water circulation on the Amundsen Shelf (Ha et al., 2014; Jacobs et al., 2011, 2012; Jenkins et al., 2010; Wåhlin et al., 2010, 2016). The intrusion of CDW onto the Amundsen Shelf over the shelf break occurs along glacier-carved troughs (Figure 1). Upon intrusion onto the shelf, physical properties of CDW are modified by mixing with the water on the shelf and the water mass becomes MCDW (Modified CDW). Upwelling of MCDW and mixing with the upper water column occur on the shelf, especially during summer (Kim et al., 2017). A portion of MCDW intrudes beneath the ice shelves, melting their base. Ultimately, waters move out of the Amundsen Sea in the upper layer (Ha et al., 2014). According to a moored ADCP (Acoustic Doppler Current Profiler) study, MCDW inflow along the western glacier-carved trough (the Dotson Trough) is ~0.3 Sv (Ha et al., 2014). Northward outflow along the western flank of the Dotson Trough (Ha et al., 2014) is about one third the magnitude of the inflow; the fate of the remaining two thirds is not yet known. If the remaining portion were to become mixed with the overlying water, its flux would be sufficient to replace the water on the western Amundsen Shelf within a few years. However, the length of time that the water stays on the Amundsen Shelf is not yet resolved.

©2018. American Geophysical Union. All Rights Reserved.

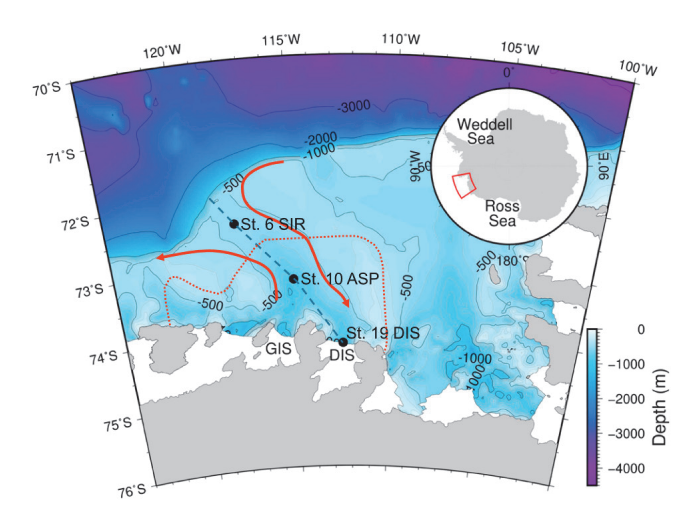


Figure 1. Bathymetry of the Amundsen Sea showing the locations of the three study sites, along the Dotson Trough (black dashed line). The red dotted line indicates the approximate boundary of the Amundsen Sea Polynya on 15 February 2012. MCDW is proposed to flow southward along the eastern flank of the Dotson Trough, with one third of this inflow moving northwestward along the western flank (indicated by solid red lines with arrows; Ha et al., 2014). SIR, ASP, and DIS denote the sea ice region, Amundsen Sea Polynya, and Dotson Ice Shelf, respectively.

Another important feature of the Amundsen Sea is the presence of highly productive polynyas, with the Amundsen Sea Polynya (ASP) reportedly being the most productive (Arrigo et al., 2012; Arrigo & van Dijken, 2003). High primary production is expected to increase absorption of atmospheric CO₂ during the austral summer. Snapshots of gas exchange rates have been obtained in the ASP during field expeditions (Mu et al., 2014; Tortell et al., 2012), but rates in the region with perennial sea ice cover (sea ice region, SIR) north of the ASP have not been well studied. Because satellite observations are not available, our understanding of primary production and gas exchange in the SIR is very limited.

The radiocarbon isotope ratio of dissolved inorganic carbon (DIC) can be used as an effective tool in examining these issues. CDW is relatively depleted in ^{14}C content ($\Delta^{14}\text{C}=-160\%$ to -150%; Bercovici & Hansell, 2016; Key & McNichol, 2012), distinctly different to atmospheric CO $_2$ in the Southern Ocean ($\Delta^{14}\text{C}$ presently +40%; Hua et al., 2013). On the Amundsen Shelf where CDW reaches the relatively shallow depth, this significant difference in $\Delta^{14}\text{C}$ between the two reservoirs facilitates its use in the examination of gas exchange rates. In this study, we applied radiocarbon-based mass balance calculations to examine the absorption rates of atmospheric CO $_2$. Based on a box model that incorporates this information, along with understood features of water circulation, we estimated the turnover time of water in the Dotson Trough region of the western Amundsen Sea.

2. Methods

Seawater samples for DIC radiocarbon measurement were collected during a cruise aboard the IBRV *Araon* in February and March 2012 in the Amundsen Sea (Figure 1 and supporting information Table S1). Samples were collected at five to eight different depths depending on water depth, at three stations along the Dotson Trough: in the sea ice region (Station 6, the *SIR site*: 72.39°S, 117.72°W; 520-m water depth; visited on 3 March 2012), in the central region of the ASP (Station 10, the *ASP site*: 73.25°S, 114.99°W; 825 m; 12 February 2012), and near the Dotson Ice Shelf within the ASP (Station 19, the *DIS site*: 74.20°S, 112.51°W; 1,065 m; 16 February 2012). Sea ice coverage at the time of sampling, as inferred from satellite data, was ~0% at the ASP and DIS sites and ~97% at the SIR site (Kim, Hwang, et al., 2015). Sampling was performed during the declining phase of a phytoplankton bloom, when average chlorophyll-*a* concentrations and average daily productivity in the ASP were significantly diminished compared with the peak bloom period (Kim, Joo, et al., 2015; La et al., 2015). Hydrographic temperature and salinity data were obtained using an SBE 911 plus CTD.

For sampling for DIC in seawater, we followed the protocol of Dickson et al. (2007). Briefly, seawater from each Niskin bottle was drained into a 500 ml Pyrex glass bottle (Duran) that had been acid washed and precombusted at 450 °C for 4 hr, and 100 μ l of saturated HgCl₂ solution was added to suppress biological activity. The bottles were capped with greased stoppers, bound with rubber bands, and stored at room temperature until analysis.

Analyses involved addition of 4.5 ml of concentrated phosphoric acid and extraction of CO_2 by bubbling N_2 gas through a closed circuit on a vacuum-line system for carbon isotope analysis (McNichol et al., 1994). Recovery of inorganic carbon was $96\% \pm 5\%$, according to multiple measurements of a working standard (n=27), a batch of surface water samples collected from the east coast of South Korea. Radioactive and stable carbon isotopic ratios were determined at the National Ocean Sciences Accelerator Mass Spectrometry Facility at Woods Hole Oceanographic Institution. The radiocarbon isotope ratio is reported as $\Delta^{14}C$ values (Stuiver & Polach, 1977).

3. Results

3.1. Hydrography

Three primary water masses were observed on the Amundsen Shelf (Figure 2; Kim, Hahm, et al., 2016). Highest potential temperatures of $0.3 \,^{\circ}\text{C}$ – $0.7 \,^{\circ}\text{C}$, close to that of MCDW, were observed at the seafloor at each site.

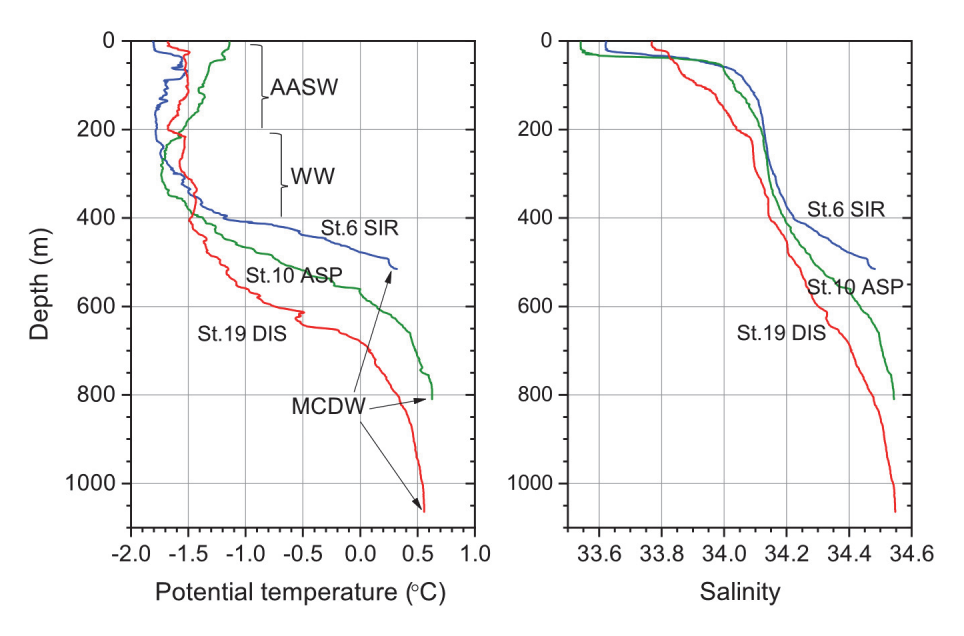


Figure 2. Vertical distribution of (left) potential temperature and (right) salinity at the three sites in this study. SIR, ASP, and DIS denote the sea ice region, Amundsen Sea Polynya, and Dotson Ice Shelf, respectively. AASW = Antarctic Surface Water; WW = Winter Water; MCDW = Modified Circumpolar Deep Water.

Potential temperature of MCDW is usually >1 °C (Wåhlin et al., 2010); therefore, the waters at the bottom were already modified further by mixing with upper water. The highest temperature at the SIR site was slightly lower than those at the other sites. Winter Water (WW) exhibits the lowest potential temperature and occupies a middle layer of variable thickness at depths of 200–400 m. WW is a cold water mass formed through sea ice production during the previous winter (Figure S1). We observed a rapid rise in temperature with increasing depth in the layer between WW and MCDW, potentially reflecting mixing between the two water masses. Antarctic Surface Water (AASW), which is influenced by seasonal warming and freshening during the summer, was present above the WW layer. Temperature gradually increased toward the surface in this layer at the ASP site, whereas the temperature was relatively uniform at the other sites.

Salinity changed sharply at a depth of about 40 m at the SIR and ASP sites because of sea ice melting (Figure 2). In contrast, salinity gradually decreased from the bottom upward at the DIS site where sea surface salinity was highest. Vertical distributions of density (not shown) were similar to those of salinity. A surface mixed layer of ~40 m thickness was apparent at the SIR and ASP sites.

3.2. Carbon Isotope Measurements

The Δ^{14} C values of DIC varied within a relatively narrow range of -129% to -162% (Figure 3 and Table S1), and the uncertainty in Δ^{14} C measurements was therefore critical. We analyzed two sets of duplicate samples (810 m depth at the ASP site and 410 m depth at the DIS site) and compared measurements from two sets of samples collected from adjacent depths (surface and 20 m were within the surface mixed layer, at the ASP site; 1,020 and 1,064 m within the layer of uniform density, at the DIS site). The average difference between each of the four pairs was $1.8\% \pm 1.7\%$. Based on this agreement and an analytical AMS uncertainty of $\sim 3\%$ (McNichol et al., 1994), we assigned a measurement uncertainty of $\pm 5\%$.

The δ^{13} C values of these four pairs agreed within 0.4‰, except for one sample: the value at 410 m depth at the DIS site, -0.6‰, was lower than those of its duplicate and adjacent samples. The incomplete transfer of extracted CO₂ (only ~30%) during sample handling, and consequent isotopic fractionation, might account for this disparity. However, the measured Δ^{14} C value was the same as that of a duplicate analysis (-146‰), as expected because Δ^{14} C values are corrected for isotopic fractionation (Stuiver & Polach, 1977).

At the SIR and ASP sites, DIC Δ^{14} C values were -154% to -147% and -161% to -129%, respectively (Figure 3), with the highest surface Δ^{14} C value of the three sites being recorded at the latter (-136%). At

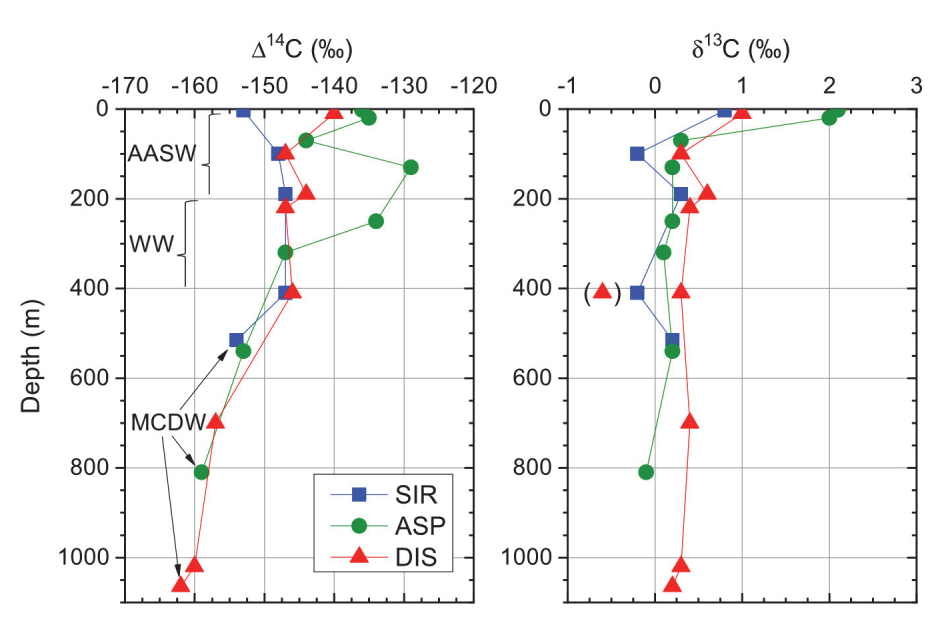


Figure 3. Vertical distribution of (left) Δ^{14} C values and (right) δ^{13} C values in per mil (‰) at the three sites in the Amundsen Sea. The δ^{13} C value in parentheses is an outlier (see section 3.2).

the ASP site, Δ^{14} C values decreased to -144% at 70 m depth, and the highest values, -129% and -134%, were observed at depths of 130 and 250 m, respectively. Below 400 m, Δ^{14} C values decreased with increasing depth. At the DIS site, the Δ^{14} C values generally decreased downward from surface to bottom, from -140% to -162% (Figure 3). Values within the 100–400 m middle layer were virtually identical.

At all sites, δ^{13} C values varied vertically within a narrow range of <0.5‰, with the exception at the surface where the values were significantly higher (Figure 3). Surface values were highest at the ASP site and lowest at the SIR site.

4. Discussion

4.1. Processes Affecting DIC Δ^{14} C Values on the Amundsen Shelf

Below ~400 m depth at all three sites, Δ^{14} C values exhibit a decreasing trend with increasing depth (Figure 3). Values near the seafloor at the ASP and DIS sites are similar to those measured in the lower ($-152\% \pm 8\%$) and upper CDW ($-159\% \pm 6\%$) at latitude 67°S (Bercovici & Hansell, 2016; Sabine et al., 2012). The deepest value at the SIR site is similar to values from corresponding depths at the other two sites, implying that the water at the seafloor there is slightly modified by mixing with shelf water (Kim, Hahm, et al., 2016), as also reflected by slightly lower temperatures and salinities than at the other sites. The vertical distribution of Δ^{14} C values in the water column below the WW layer at the three sites could be explained by MCDW intrusion and mixing with WW. Δ^{14} C values at 100–410 m are virtually identical at all sites ($-147\% \pm 1\%$; n=8), with the exception of values at 130 and 250 m at the ASP site (Figure 3). Δ^{14} C values in the surface mixed layer are higher than the values from immediately below the surface mixed layer except for the SIR site. The recording of highest surface values at the ASP site suggests that absorption of atmospheric CO₂ was the cause of the increase in Δ^{14} C.

Other processes may also affect DIC Δ^{14} C values, such as remineralization of POC (particulate organic carbon), input from glacial meltwater, and flux from sediments. In the open ocean, there is reportedly too little remineralization of sinking POC to cause any significant increase in DIC Δ^{14} C values (Druffel et al., 2003). In a conservative case, where half of the annual primary production (half of ~80 g C m⁻² yr⁻¹, equivalent to 3.3 mol m⁻² yr⁻¹; Arrigo et al., 2012) is exported and remineralized in the upper 400 m of the water column (where most respiration occurs), carbon export would constitute only 0.4% of the DIC present in that water column ((3.3 mol m⁻²)/(2.215 mol m⁻³ × 400 m) × 100(%) = 0.4%; DIC concentration is from Yager et al., 2016). Furthermore, the similarity in the DIC Δ^{14} C values of MCDW (–160‰)

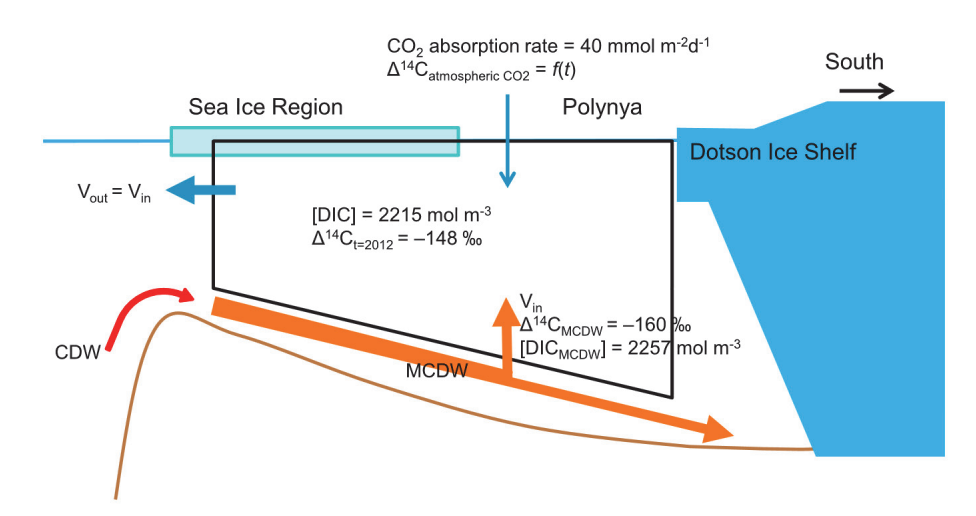


Figure 4. Schematic layout of the box model. Part of the Modified CDW (MCDW) mixes with the overlying water along the Dotson Trough ($V_{\rm in}$), while and an equal volume of water ($V_{\rm out}$) leaves the box carrying any excess dissolved inorganic carbon (DIC). Sources of radiocarbon to the box include the input of MCDW and absorption of atmospheric CO₂ (Turnbull et al., 2017). Yearly changes in the DIC Δ^{14} C of the box occur by mixing with these sources and are calculated based on radiocarbon mass balance.

and freshly produced POC (-144%; Kim, Hwang, et al., 2016) means that the effect of remineralization on DIC Δ^{14} C value would be negligible.

Regarding glacial meltwater, its content in seawater is estimated to be 0.3%–0.8% along the Dotson Trough (Kim, Hahm, et al., 2016). Based on the properties of the Byrd ice core at depths of 1,068–1,469 m (average gas content = 110 cm³ kg $^{-1}$ at 0 °C and 1 atm; average CO $_2$ abundance = 0.027%; Fireman & Norris, 1982), the CO $_2$ content in the glacier is ~1.3 µmol C kg $^{-1}$. The 14 C age of the Byrd ice core at 1,071 m depth is >8,000 yr (Δ^{14} C < -630%; Fireman & Norris, 1982). Based on this information, radiocarbon mass balance calculations indicate that changes in Δ^{14} C caused by glacial meltwater would be <1%. The carbon flux from sediments to the overlying water column was estimated from published data for nutrient fluxes from sediment at the ASP site (0.13 mmol N m $^{-2}$ d $^{-1}$ and 0.017 mmol P m $^{-2}$ d $^{-1}$; Kim, Choi, et al., 2016) and a Redfield stoichiometry. The carbon flux was ~0.8 mol m $^{-2}$ yr $^{-1}$, corresponding to only ~0.1% of the DIC inventory of the ~300 m thick bottom layer.

The Δ^{14} C values at the SIR site ($-149\% \pm 2\%$, n=4; Table S1), measured in the WW and AASW layers, are much lower than those of the outer Southern Ocean (-102%; Sabine et al., 2012). This implies that water in the upper layer of the western Amundsen Sea originated from modification of MCDW rather than inflow from the outer shelf. This scenario is consistent with the modeled circulation of Kim et al. (2017), in which MCDW flows coastward along the seafloor and cold upper water flows northward off the shelf (see Figure 9 of Kim et al., 2017), and also with the findings of ADCP and LADCP (Lowered ADCP) surveys conducted on the western Amundsen Shelf (Ha et al., 2014).

4.2. Absorption of Atmospheric CO₂ by Gas Exchange

 Δ^{14} C values of the surface mixed layer at the ASP site are higher than those at the other sites implying a greater input of CO₂ at this site. Absorption of atmospheric CO₂ in the central polynya is increased by high primary production with a consequent low surface water pCO₂ (Mu et al., 2014; Tortell et al., 2012). Satellite data indicate highest chlorophyll-a concentrations in the central region of the ASP and much lower values at the periphery and near the DIS (La et al., 2015). The intensity of primary production is reflected by the distribution of δ^{13} C in the surface mixed layer. Higher δ^{13} C values at the surface than at deeper depths are caused by biological fractionation during primary production (Fischer, 1991; Masiello et al., 1998). The highest δ^{13} C value at the ASP site (Figure 3) is consistent with satellite observations and in situ measurements of primary production in the Amundsen Sea (Lee et al., 2017).

The pCO₂ values in surface waters exhibit a similar spatial distribution to that of primary production, but in the opposing direction (Mu et al., 2014). Although observed at different times, in situ measurements of



 pCO_2 also support greater rates of CO_2 absorption in the central ASP where values as low as 80 μ atm were recorded in January–February 2009 (Tortell et al., 2012) and 130 μ atm in December 2010 to January 2011 (Mu et al., 2014). In contrast, pCO_2 values near the DIS were near equilibrium or even supersaturated with respect to the atmosphere (Mu et al., 2014).

If initial conditions before air-sea exchange (commencing in spring and summer) could be determined, the difference between the measured and initial Δ^{14} C values would provide an independent estimate of CO₂ absorption rate (Broecker et al., 1985). This would provide a time-integrated value of net CO₂ absorption between the initiation of gas exchange and the time of sampling. No radiocarbon data for the Amundsen Sea during the austral winter or at the start of polynya opening were available, so we estimated initial values on the basis of current understanding of water circulation. WW, which overlies MCDW, is a cold (near-freezing), less saline water mass formed through sea ice production during the previous winter (Yager et al., 2012). In spring, when the sea ice starts to melt and the polynya opens, AASW forms by freshening and warming of WW (Tortell et al., 2012). In late summer, as the open-water region shrinks, AASW cools to freezing and becomes saline due to sea ice formation, eventually returning to WW. Therefore, we assumed that the initial Δ^{14} C value of surface water is equal to that of WW (average $-146\% \pm 1\%$; six results between 190 and 410 m were used except for the high value at 250 m, at the ASP site) and used the difference in Δ^{14} C values between surface water and WW to estimate rates of CO₂ absorption into the 40-m-thick surface mixed layer. At the ASP and DIS sites, the rates of CO_2 absorption averaged over 120 days of polynya opening were 45 ± 20 and 28 ± 20 mmol m⁻² d⁻¹ (the uncertainties are propagated errors), respectively. A surface water Δ^{14} C value lower than the WW layer at the SIR site cannot be explained by either CO₂ absorption or release, although the values are not significantly different considering the uncertainty of $\pm 5\%$.

These exchange rate estimates are similar to values determined by in situ measurements and modeling, as follows: continuous measurements of pCO_2 in surface water, December–January, indicate spatially averaged CO_2 fluxes of ~18 mmol m⁻² d⁻¹ over the entire open-water region and ~36 mmol m⁻² d⁻¹ in the central ASP (Mu et al., 2014); Tortell et al. (2012) estimated a mean sea-air flux of 42 mmol m⁻² d⁻¹ in open polynya waters; Arrigo et al. (2008) used modeling to estimate an absorption rate of 46–71 mmol m⁻² d⁻¹ during the bloom period in the Ross Sea; and an estimate based on radiocarbon measurements in the Weddell Sea is 60 mmol m⁻² d⁻¹ (Weiss et al., 1979).

High Δ^{14} C values were observed at the ASP site at depths of 130 and 250 m, and it is not clear whether they represent remnants of accumulation from previous years. Considering a turnover time of a few decades (section 4.3), it is possible that Δ^{14} C values in the WW layer at the ASP site were higher than those in the other regions. In that case, more rapid mixing in the surface water than in the WW layer would be required to explain the low value at 70 m depth. Sea ice movement in winter may cause such rapid mixing near the surface (Kim et al., 2017), but further research is required to determine whether this is a persistent phenomenon.

4.3. Turnover Time of Water on the Amundsen Shelf

The time required for the increase in Δ^{14} C values in the entire water column over that of MCDW (i.e., the lowest Δ^{14} C value observed, -162%) via absorption of CO₂ may be considered as the turnover time of water. A simple one-box model was adopted to determine the turnover time that best explains the observed vertical profile of Δ^{14} C values (Figure 4; see supporting information for details), with boundaries set as a region along the Dotson Trough (volume 2.46×10^{13} m³, Figures 4 and S2; Wessel et al., 2013). The input of radiocarbon to the box incorporates inflow of MCDW and absorption of atmospheric CO₂ via gas exchange. The Δ^{14} C value integrated over the Dotson Trough region (the DIC reservoir) was calculated from the radiocarbon mass balance between newly introduced sources and the existing DIC reservoir. The calculated Δ^{14} C value for the DIC reservoir was used as the new value for the next year's calculation. Temporal variations in Δ^{14} C values for the DIC reservoir between 1965 and 2012 were calculated for turnover times of 5–100 years. Here turnover time is defined as the ratio of total water volume in the box to the fraction of the intruding MCDW that becomes mixed with the overlying water (Figure 4). The initial Δ^{14} C value for the DIC reservoir was calculated by iteration with a fixed Δ^{14} C value for atmospheric CO₂ (0‰) until the value reached a steady state. The estimated Δ^{14} C value for the DIC reservoir increased with time to a maximum then decreased (Figure S3). The maximum value and the time at which it was reached are dependent on turnover time. The Δ^{14} C value for the DIC reservoir in 2012 increased as the turnover time increased. Using this model approach, we



reproduced the observed Δ^{14} C value of -148%, integrated over the entire water column, with turnover times of 10–30 years (Figure S3).

5. Summary

Based on measured Δ^{14} C values of DIC and our box model results, we estimate that it takes 10–30 years for the turnover of the water in the Dotson Trough region. A previous study of water flow along the Dotson Trough demonstrated that about one third of inflowing MCDW exits in the Amundsen Shelf along the trough (see arrows in Figure 1; Ha et al., 2014). Those authors suggested that the remainder flows through uncharted troughs in the west, westward along the coast, or upward to the surface layer (Ha et al., 2014). Our estimated turnover time implies that a significantly smaller fraction (9%–26%) of the intruding MCDW flux (~0.3 Sv) mixes with the overlying water, with the fate of the remainder remaining unclear. Moreover, the turnover time estimate for the Dotson Trough region is significantly longer than that of the Ross Sea (~6 years; Sweeney, 2013). Presumably, both the shallow shelf break and coastward deepening of the seafloor restrict the inflow of water from off-shelf regions and prevent rapid turnover in the western Amundsen Sea. Understanding the fate of MCDW in the Amundsen Sea is important to advancing our understanding of key processes, such as melting of the ice shelves and sea ice, and nutrient supply to the pelagic ecosystem. Our estimate of turnover time is the first of its kind in the Amundsen Sea. Further research using other tracers such as chlorofluorocarbons (Trumbore et al., 1991) will complement this preliminary estimate.

Acknowledgments

We thank Dr. Tae Wan Kim for the hydrographic data and his help with station map preparation, staff at NOSAMS for carbon isotope measurements, and the captain and crew of the IBRV Araon for their assistance at sea. This study was supported by the Korea Polar Research Institute (PP 17020). The carbon isotope data used are listed in the supporting information. We acknowledge the use of Δ^{14} C results for atmospheric CO₂ measured at Baring Head, New Zealand (data were downloaded from https:// www.niwa.co.nz/atmosphere/our-data/ trace-gas-plots/carbon-dioxide). Temperature and salinity data presented are available at https://figshare. com/s/4bec98267fb252dd9067.

References

- Arrigo, K. R., Lowry, K. E., & Van Dijken, G. (2012). Annual changes in sea ice and phytoplankton in polynyas of the Amundsen Sea, Antarctica. *Deep Sea Research Part II: Topical Studies in Oceanography*, 71, 5–15.
- Arrigo, K. R., & Van Dijken, G. (2003). Phytoplankton dynamics within 37 Antarctic coastal polynya systems. *Journal of Geophysical Research*, 108(C8), 3271. https://doi.org/10.1029/2002JC001739
- Arrigo, K. R., Van Dijken, G., & Long, M. (2008). Coastal Southern Ocean: A strong anthropogenic CO₂ sink. *Geophysical Research Letters*, 35, L21602. https://doi.org/10.1029/2008GL035624
- Bercovici, S. K., & Hansell, D. A. (2016). Dissolved organic carbon in the deep Southern Ocean: Local versus distant controls. *Global Biogeochemical Cycles*, 30, 350–360. https://doi.org/10.1002/2015GB005252
- Broecker, W. S., Peng, T. H., Ostlund, G., & Stuiver, M. (1985). The distribution of bomb radiocarbon in the ocean. *Journal of Geophysical Research*, 90(C4), 6953–6970. https://doi.org/10.1029/JC090iC04p06953
- Dickson, A. G., Sabine, C. L., & Christian, J. R. (Eds.) (2007). *Guide to best practices for ocean CO*₂ measurements, PICES Special Publication (Vol. 3). North Pacific Marine Science Organization.
- Druffel, E. R. M., Bauer, J. E., Griffin, S., & Hwang, J. (2003). Penetration of anthropogenic carbon into organic particles of the deep ocean. Geophysical Research Letters, 30(14), 1744. https://doi.org/10.1029/2003GL017423
- Fireman, E. L., & Norris, T. L. (1982). Ages and composition of gas trapped in Allan Hills and Byrd core ice. *Earth and Planetary Science Letters*, 60(3), 339–350. https://doi.org/10.1016/0012-821X(82)90072-3
- Fischer, G. (1991). Stable carbon isotope ratios of plankton carbon and sinking organic matter from the Atlantic sector of the Southern Ocean. *Marine Chemistry*, 35(1–4), 581–596. https://doi.org/10.1016/S0304-4203(09)90044-5
- Ha, H. K., Wåhlin, A. K., Kim, T. W., Lee, S. H., Lee, J. H., Lee, H. J., et al. (2014). Circulation and modification of warm deep water on the central Amundsen Shelf. *Journal of Physical Oceanography*, 44(5), 1493–1501. https://doi.org/10.1175/JPO-D-13-0240.1
- Hua, Q., Barbetti, M., & Rakowski, A. Z. (2013). Atmospheric radiocarbon for the period 1950–2010. Radiocarbon, 55(04), 2059–2072. https://doi.org/10.2458/azu_js_rc.v55i2.16177
- Jacobs, S. S., Jenkins, A., Giulivi, C. F., & Dutrieux, P. (2011). Stronger ocean circulation and increased melting under Pine Island Glacier ice shelf. *Nature Geoscience*, 4(8), 519–523. https://doi.org/10.1038/ngeo1188
- Jacobs, S. S., Jenkins, A., Hellmer, H., Giulivi, C., Nitsche, F., Huber, B., & Guerrero, R. (2012). The Amundsen Sea and the Antarctic ice sheet. Oceanography, 25(3), 154–163. https://doi.org/10.5670/oceanog.2012.90
- Jenkins, A., Dutrieux, P., Jacobs, S. S., McPhail, S. D., Perrett, J. R., Webb, A. T., & White, D. (2010). Observations beneath Pine Island Glacier in West Antarctica and implications for its retreat. *Nature Geoscience*, 3(7), 468–472. https://doi.org/10.1038/ngeo890
- Key, R. M., & McNichol, A. P. (2012). Radiocarbon measurements in the Indian Ocean aboard RVIB Nathaniel B. Palmer. *Oceanography*, 25(3), 152–153. https://doi.org/10.5670/oceanog.2012.89
- Kim, B. K., Joo, H., Song, H. J., Yang, E. J., Lee, S., Hahm, D., Rhee, T. S., et al. (2015). Large seasonal variation in phytoplankton production in the Amundsen Sea. *Polar Biology*, 38(3), 319–331. https://doi.org/10.1007/s00300-014-1588-5
- Kim, I., Hahm, D., Rhee, T. S., Kim, T. W., Kim, C. S., & Lee, S. (2016). The distribution of glacial meltwater in the Amundsen Sea, Antarctica, revealed by dissolved helium and neon. *Journal of Geophysical Research: Oceans, 121*, 1654–1666. https://doi.org/10.1002/2015JC011211
- Kim, M., Hwang, J., Kim, H. J., Kim, D., Yang, E. J., Ducklow, H. W., et al. (2015). Sinking particle flux in the sea ice zone of the Amundsen shelf, Antarctica. *Deep Sea Research Part I: Oceanographic Research Papers*, 101, 110–117. https://doi.org/10.1016/j.dsr.2015.04.002
- Kim, M., Hwang, J., Lee, S. H., Kim, H. J., Kim, D., Yang, E. J., & Lee, S. (2016). Sedimentation of particulate organic carbon on the Amundsen Shelf, Antarctica. Deep Sea Research Part II: Topical Studies in Oceanography, 123, 135–144. https://doi.org/10.1016/j.dsr2.2015.07.018
- Kim, S.-H., Choi, A., Yang, E. J., Lee, S., & Hyun, J.-H. (2016). Low benthic respiration and nutrient flux at the highly productive Amundsen Sea Polynya, Antarctica. Deep Sea Research Part II: Topical Studies in Oceanography, 123, 92–101. https://doi.org/10.1016/j.dsr2.2015.10.004
- Kim, T. W., Ha, H. K., Wåhlin, A. K., Lee, S. H., Kim, C. S., Lee, J. H., & Cho, Y. K. (2017). Is Ekman pumping responsible for the seasonal variation of warm circumpolar deep water in the Amundsen Sea? *Continental Shelf Research*, 132, 38–48. https://doi.org/10.1016/j.csr.2016.09.005



- La, H. S., Lee, H., Fielding, S., Kang, D., Ha, H. K., Atkinson, A., et al. (2015). High density of ice krill (Euphausia crystallorophias) in the Amundsen Sea coastal polynya, Antarctica. *Deep Sea Research Part I: Oceanographic Research Papers*, 95, 75–84. https://doi.org/10.1016/j. dsr.2014.09.002
- Lee, S., Hwang, J., Ducklow, H. W., Hahm, D., Lee, S. H., Kim, D., et al. (2017). Evidence of minimal carbon sequestration in the productive Amundsen Sea Polynya. *Geophysical Research Letters*, 44, 7892–7899. https://doi.org/10.1002/2017GL074646
- Masiello, C. A., Druffel, E. R. M., & Bauer, J. E. (1998). Physical controls on dissolved inorganic radiocarbon variability in the California Current. Deep-Sea Research Part II, 45(4-5), 617–642. https://doi.org/10.1016/S0967-0645(97)00096-9
- McNichol, A. P., Jones, G. A., Hutton, D. L., Gagnon, A. R., & Key, R. M. (1994). The rapid preparation of seawater ΣCO₂ for radiocarbon analysis at the National Ocean Sciences AMS Facility. *Radiocarbon*, *36*(02), 237–246. https://doi.org/10.1017/S0033822200040522
- Mu, L., Stammerjohn, S. E., Lowry, K. E., & Yager, P. L. (2014). Spatial variability of surface pCO₂ and air-sea CO₂ flux in the Amundsen Sea Polynya, Antarctica. *Elementa: Science of the Anthropocene*, 3, 36.
- Pritchard, H. D., Ligtenberg, S. R. M., Fricker, H. A., Vaughan, D. G., Van den Broeke, M. R., & Padman, L. (2012). Antarctic ice-sheet loss driven by basal melting of ice shelves. *Nature*, 484, 502–505. https://doi.org/10.1038/nature10968, 7395.
- Rignot, E., Mouginot, J., Morlighem, M., Seroussi, H., & Scheuchl, B. (2014). Widespread, rapid grounding line retreat of Pine Island, Thwaites, Smith, and Kohler glaciers, West Antarctica, from 1992 to 2011. *Geophysical Research Letters*, 41, 3502–3509. https://doi.org/10.1002/2014GI
- Sabine, C., Feely, R., Wanninkhof, R., Dickson, A., Millero, F., Hansell, D., et al. (2012). Carbon dioxide, hydrographic, and chemical data obtained during the R/V Nathaniel B. Palmer cruise in the Southern Ocean on CLIVAR repeat hydrography section S04P (Feb. 19–Apr. 23, 2011). Carbon Dioxide Information Analysis Center, Oak Ridge National. Laboratory, US Department of Energy, Oak Ridge, Tennessee. https://doi.org/10.3334/CDIAC/OTG.CLIVAR_S04P_2011
- Stammerjohn, S., Massom, R., Rind, D., & Martinson, D. (2012). Regions of rapid sea ice change: An inter-hemispheric seasonal comparison. Geophysical Research Letters, 39, L06501. https://doi.org/10.1029/2012GL050874
- Geophysical Research Letters, 39, L06501. https://doi.org/10.1029/2012GL050874

 Stuiver, M., & Polach, H. A. (1977). Discussion reporting of ¹⁴C data. Radiocarbon, 19(03), 355–363. https://doi.org/10.1017/S0033822200003672
- Sweeney, C. (2013). The annual cycle of surface water CO₂ and O₂ in the Ross Sea: A model for gas exchange on the continental shelves of Antarctica. *Biogeochemistry of the Ross Sea*, 78, 295–312.
- Tortell, P. D., Long, M. C., Payne, C. D., Alderkamp, A.-C., Dutrieux, P., & Arrigo, K. R. (2012). Spatial distribution of pCO₂, ΔO₂/Ar and dimethylsulfide (DMS) in polynya waters and the sea ice zone of the Amundsen Sea, Antarctica. *Deep Sea Research Part II: Topical Studies in Oceanography*, 71, 77–93.
- Trumbore, S. E., Jacobs, S. S., & Smethie, W. M. Jr. (1991). Chlorofluorocarbon evidence for rapid ventilation of the Ross Sea. *Deep Sea Research Part A. Oceanographic Research Papers*, 38(7), 845–870. https://doi.org/10.1016/0198-0149(91)90022-8
- Turnbull, J. C., Mikaloff Fletcher, S. E., Brailsford, G. W., Moss, R. C., Norris, M. W., & Steinkamp, K. (2017). Sixty years of radiocarbon dioxide measurements at Wellington, New Zealand: 1954–2014. *Atmospheric Chemistry and Physics*, 17(23), 14,771–14,784. https://doi.org/10.5194/acp-17-14771-2017
- Wåhlin, A. K., Kalén, O., Assmann, K. M., Darelius, E., Ha, H. K., Kim, T. W., & Lee, S. H. (2016). Subinertial oscillations on the Amundsen Sea shelf, Antarctica. *Journal of Physical Oceanography*, 46(9), 2573–2582. https://doi.org/10.1175/JPO-D-14-0257.1
- Wåhlin, A. K., Yuan, X., Björk, G., & Nohr, C. (2010). Inflow of warm Circumpolar Deep Water in the central Amundsen Shelf. *Journal of Physical Oceanography*, 40(6), 1427–1434. https://doi.org/10.1175/2010JPO4431.1
- Walker, D. P., Brandon, M. A., Jenkins, A., Allen, J. T., Dowdeswell, J. A., & Evans, J. (2007). Oceanic heat transport onto the Amundsen Sea shelf through a submarine glacial trough. *Geophysical Research Letters*, 34, L02602. https://doi.org/10.1029/2006GL028154
- Weiss, R. F., Östlund, H. G., & Craig, H. (1979). Geochemical studies of the Weddell Sea. Deep Sea Research Part A. Oceanographic Research Papers, 26(10), 1093–1120. https://doi.org/10.1016/0198-0149(79)90059-1
- Wessel, P., Smith, W. H. F., Scharroo, R., Luis, J., & Wobbe, F. (2013). Generic mapping tools: Improved version released. *Eos, Transactions American Geophysical Union*, 94(45), 409–410. https://doi.org/10.1002/2013EO450001
- Yager, P. L., Sherrell, L., Stammerjohn, S. E., Alderkamp, A.-C., Schofield, O., Abrahamsen, E. P., et al. (2012). ASPIRE: The Amundsen Sea Polynya international research expedition. *Oceanography*, 25(3), 40–53. https://doi.org/10.5670/oceanog.2012.73
- Yager, P. L., Sherrell, R. M., Stammerjohn, S. E., Ducklow, H. W., Schofield, O. M. E., Ingall, E. D., et al. (2016). A carbon budget for the Amundsen Sea Polynya, Antarctica: Estimating net community production and export in a highly productive polar ecosystem. *Elementa: Science of the Anthropocene*, 4, 140.